Supplementary Information for

Single molecule analysis of endogenous β-actin mRNA trafficking reveals a mechanism for compartmentalised mRNA localisation in axons

Benita Turner-Bridger[1], Maximillian Jakobs[1], Leila Muresan[1], Hovy Ho-Wai Wong[1], Kristian Franze[1], William A. Harris[1], and Christine E. Holt[1]*

[1]Department of Physiology, Development and Neuroscience, University of Cambridge, Cambridge, CB2 3DY, United Kingdom.

This PDF file includes:

- Supplementary Information S1 (mathematical modelling)
- Supplementary Materials and Methods
- Legends for Supplementary Figures
- Legends for Supplementary Movies
- Supplemental References
- Supplementary Figures S1-S6
- Table S1

www.pnas.org/cgi/doi/10.1073/pnas.1806189115

SUPPLEMENTAL INFORMATION

S1. Mathematical modelling of axonal mRNA trafficking

For assessing the contribution of diffusive motion in axonal trafficking of β-actin mRNA to the tip of the axon, we used the mean square displacement equation:

$$MSD = q_i D t$$

Rearranging this equation to calculate the time it would take an mRNA to traverse the length of the axon ($MSD = L^2$) through diffusion alone gives:

$$\frac{L^2}{q_i D} = t$$

In these equations, *MSD* is the mean square displacement, $q_i = 2 \cdot dim$ (in this case 2 for 1D), *D* = the diffusion coefficient (0.03μm^2 sec^{-1} from our data for β-actin mRNA in axon shafts). *L* = the length of the axon in the optic tract (500 μm). Using our data from β-actin mRNA dynamics in axon shafts, we arrive at a time period *t* = 48 days for an mRNA to reach the tip of the axon by diffusion.

To test whether the observed velocity differences for anterograde and retrograde directed transport can yield the increased localisation in the GC, we calculated the expected fold increase with an advection-diffusion model. In this model the change in particle density $\mathrm{n(x,t)}$ at point t and position x is:

$$\partial_{\mathrm{t}}\mathrm{n(x,t)} = \mathrm{D}\,\partial_{\mathrm{x}}^2\mathrm{n(x,t)} - \mathrm{v}\,\partial_{\mathrm{x}}\mathrm{n(x,t)} - \mathrm{rn(x,t)}$$

Here D is the RNP diffusion constant, v is the average RNP velocity, and r their degradation rate. In the following we will replace r by the RNP half-life T in exponential decay: $\mathrm{r} = \ln(2)/\mathrm{T}$. As mentioned above, diffusion is irrelevant on the length scale of the axon ($> 10\mathrm{um}$) so that we can omit the first term ($\mathrm{D}\,\partial_{\mathrm{x}}^2\mathrm{n(x,t)} \approx 0$). The stationary solution ($\partial_{\mathrm{t}}\mathrm{n(x,t)} = 0$) of the resulting differential equation is:

$$\mathrm{n(x)} = \mathrm{n_0 e}^{-\frac{\ln(2)}{\mathrm{vT}}\mathrm{x}}$$

$\mathrm{n_0}$ is the RNP density at position $\mathrm{x} = 0$ which we define as $30\mu\mathrm{m}$ prior the GC (see cartoon) and v the average RNP velocity. In the next step, we assume that any RNP

with position $x > 30\mu m$ is in the GC. To calculate the fold change f we then divide the number of expected RNPs in the growth cone N_{gc} by the number of RNPs in the shaft N_{shaft}.

$$f := \frac{N_{gc}}{N_{shaft}} = \frac{n_0 \int_{30}^{\infty} dx\ e^{-\frac{r}{v}x}}{n_0 \int_{0}^{30} dx\ e^{-\frac{r}{v}x}} = \frac{1}{2^{\frac{30}{Tv}} - 1}$$

Our RNP analysis shows that about 50/50% of RNPs move antero-/retrogradely with average velocity $1.04 \pm 0.08\mu m/sec$ and $0.81 \pm 0.05\mu m/sec$ so that the average velocity of a moving particle becomes $v_{mov} = 0.12 \pm 0.05\mu m/sec$ (Errors are s.e.m.). However, only 0.079 ± 0.018 of all RNPs are moving non-diffusively in the axonal shaft at a given time and only 0.012 ± 0.055 (0.008 ± 0.052) do so in the growth cone central domain (periphery). This implies that, the average fraction of moving granules in the region of our analytical model is approximately the average of all three regions: 0.033 ± 0.007. Hence, the average velocity for all RNPs is: $0.033\, v_{mov} \rightarrow 0.004 \pm 0.002\mu m/sec$. Previous findings suggest that β-actin mRNA has a half-life of 8 hours (60,61). However, the survival of mRNA in RNPs might vary so that we allowed for a 50% error: $T = 8 \pm 4\ h$. Plugging $v = 0.004\mu m/sec$ and $T = 8h$ into the equation for f above we arrive at:

$$f = 4.8 \pm 3.5$$

SUPPLEMENTARY METHODS

Cloning

Brains and eyes were dissected from stage 32 *Xenopus laevis* embryos, RNA extracted using RNAeasy minikit (QIAGEN) and cDNA libraries generated using the SuperScriptIII first strand system synthesis system for RT-PCR (Life Technologies). γ-actin PCR products were generated using Sigma synthesised primers (forward: GCGGATCTGACAGCTACTG, reverse: CCCAAAACATTCTGTATGGAT) and Q5 high-fidelity polymerase (New England Biolabs), gel extraction (QIAquick Gel Extraction Kit, Quiagen) was followed by 20-minute incubation with Taq polymerase (New England Biolabs) and 0.2mM dATP for TA tail addition. Products were cloned into a pCRII-TOPO vector (Thermo Fischer Scientific) according to manufacturer's protocol. Plasmids were isolated using QIAprep Spin Miniprep Kit (Quiagen) and Sanger sequenced (Department of Biochemistry, Cambridge University). Full-length β-actin plasmid was generated as describe above but PCR products were amplified from a Venus_actb plasmid (1) using primers (forward: TACTCGGATCCGGCTCAGTGACCCGCCCGCATAGAAAGGAGACAGTCTGTGTG CGTCCAACCCTCAGATCACAATGGAAGACGATATTGCC, reverse: AAACTTATGTTGTTTCACGCGGCCGCTACGCATGCGTAGCGGCCGCGTGAAAC AACATAAGTTT) to remove the Venus sequence from full-length β-actin.

The β-actin myr-d2EGFP construct was created through the ligation of two PCR generated using Phusion high-fidelity polymerase (NEB) and the full-length β-actin plasmid and a myr-d2EGFP- β-actin 3'UTR plasmid as templates. The following primers were used to create (a) a PCR product containing a BamHI restriction site, β-actin 5'UTR, then β-actin coding sequence followed by a flexible linker region (forward 5'-3' AAGCATTATAAGCAGGATCCGGCTCAGTGACCCGCCCG, reverse 5'-3' ATACAGTCCATACAGTCCTCTTTCAGAATACAGTCCATACAGTCCATACAGTCCT

CTTTCAGAATACAGTCCATACAGTCCGAAGCATTTACGGTGGACAATTGAGGGG), (b) a PCR product containing an overlapping linker region followed by myr-d2EGFP, β-actin 3'UTR, and flanked by a XhoI restriction site (forward 5'-3' . GTATGGACTGTATTCTGAAAGAGGACTGTATGGACTGTATGGCACGGTGCTGTC CCTA, reverse 5'-3' GTAACCTAACTGAAAAAATAAAACTTATGTTGTTTCACCCTCGAGGCTTGTTCCG CATTT) (c) A final PCR product joining the first two PCR products (forward 5'-3' TAAGCAGGATCCGGCTCA, reverse 5'-3' ACAAGCCTCGAGGGTGAAA). The final PCR product was ligated into a BamHI XhoI digested PCS2+ vector using T4 DNA ligase (Thermo Fisher Scientific).

RTPCR confirmation of potential off-target for MB binding

The only off-target with 100% minus/plus base-pairing to MB2 (Fam83h-like) was confirmed not to be expressed in *Xenopus* RGC axons by performing RTPCR using RNA extracted from isolated axons using the modified Boyden chamber, as described by (2) and comparing expression to RNA extracted from whole heads of *Xenopus* (fig. S6B). The following primers were used with OneStep RTPCR Kit (QIAGEN) according to manufacturers instructions: β-actin (positive control): forward 5'-3' CCTGTGCAGGAAGATCACAT, reverse 5'-3' TGTTAAAGAGAATGAGCCCC; Map2 (negative control): forward 5'-3' CGATCATCCTTGCCAAGACCTTCCTC, reverse 5'-3' GCGACCTGGAGATTGGGTGATGATTT; GluR1 (negative control) forward 5'-3' GGGATTGGCCATGCTTGTTG, reverse 5'-3' GCCATTCCTGCACTGTGGCTCA; Fam83h-like (encompassing all three transcript variants): forward 5'-3' GCTATCGATGTTCTGGCGGA, reverse 5'-3'TGGGCAATGCTGCGATGTAT.

In vitro transcription

Fluorescently-tagged capped mRNA were synthesised from sense linearized full-length β-actin plasmids by SP6-RNA polymerase (Roche). *In vitro* transcription was performed using Cy5-UTP (PerkinElmer) as previously described (3).Transcription products were purified using the RNeasy Mini Kit (Qiagen) precipitated overnight with lithium chloride (Ambion), then resuspended in RNAase-free water. Unlabelled mRNA for MB validation was *in vitro* transcribed using mMESSAGE mMACHINE SP6 Transcription Kit (Life Technologies) according to the manufacturer's protocol.

Colocalisation analysis

Cy5-UTP β-actin mRNA and Cy5-UTP γ-actin mRNA were imaged together with MB1 and MB2 targeting β-actin mRNA in primary RGC axons within 22 hours of electroporation. Images were acquired on an Olympus IX81 inverted microscope equipped with a PerkinElmer Spinning Disk UltraVIEW VoX and a 100x (1.4 N.A., Nikon oil immersion objective with an ORCA-Flash4.0 V2 CMOS camera (Hamamatsu) using Volocity 6.3.0 software (PerkinElmer). Cy5-UTP exogenous mRNA was imaged using a 641nm laser line set at 19.5 % laser intensity and 200ms exposure time, β-actin MBs were imaged using a 560 nm laser line at 27% intensity and 200ms exposure time. Images were acquired at 0.5 time-points per second for 20 frames. Colocalisation was assessed using Volocity visualisation software. MB and Cy5-UTP mRNA were counted as colocalised if two puncta overlapped and travelled together for the duration of the movie, or until photobleaching occurred (minimum of 5 frames). To avoid bias in total number of puncta colocalised within a population of variable expression levels, we analysed colocalisation in 20μm sections of axon shafts with similar ratios of Cy5-UTP mRNA and MBs co-expressed (0.8-1.2 Cy5-UTP puncta to MB puncta).

For MB:β-actin mRNA smFISH colocalisation, three non-simultaneous images were taken of the same axons using the same microscope: one of MBs immediately after fixation, one after bleaching the MB signal using an UltraVIEW PhotoKinesis device (PerkinElmer) - to ensure no signal would transfer to smFISH images, and finally an image was taken after performing the smFISH protocol against β-actin mRNA (see section below). Colocalisation between MBs in the first, and β-actin mRNA smFISH in the last image, was estimated using a custom-built Matlab script. In the script, puncta in the last image were mapped to the first using axon morphology in the bright-field channel to register movement and deformation during the smFISH protocol. A detailed workflow for the script is provided in supplementary materials. Vg1RBP-EGFP puncta immediately post-fixation were registered to immunohistochemistry (IHC) against GFP as a positive control. As a negative control, Vg1RBP-EGFP colocalisation was estimated with puncta in the IHC image that had been randomised.

Immunohistochemistry (IHC)

For assessing the performance of our bright-field registration script, we performed IHC against EGFP following a sham smFISH protocol (i.e. with no smFISH probes added to hybridization solution) to mimic axon deformations generated by washes and heat during smFISH hybridization. Immunohistochemistry against Vg1RBP-EGFP was subsequently performed as depicted previously (4) using an anti-GFP primary antibody (ab6556, 1:1500) and Alexa Fluor 647 goat anti-rabbit secondary antibody (Life Technologies).

To evaluate how MB hybridization to β-actin mRNA might affect β-actin protein synthesis, we captured live images of axons containing MBs, then performed IHC against β-actin protein as described (4) using 10 min incubation in ice-cold methanol for fixation, and a FITC-conjugated β-actin primary antibody (ab6277, 1:200). The

same axons were identified from the previous live images, and captured on the spinning disk microscope setup (described above) using a 488nm laser line at 23.5% intensity and 50ms exposure time, live MB images were acquired using a 561nm laser line at 27% laser intensity with 300ms exposure time. Immunofluorescence was measured using Volocity 6.3.0 (PerkinElmer) with the growth cone ROI identified in the bright-field channel. Normalised fluorescence intensity was calculated by subtracting the background from an equivalently sized ROI immediately next to the growth cone.

Stepwise photobleaching

Stage 28 eye primordia were electroporated with 50μM MB1 and cultured for 18-22 hours. Explant cultures were fixed for 10 mins in 4%w/v PFA, washed once in 4% sucrose-1XPBS, then 3x in 1XPBS. Photobleaching was performed in 1XPBS via highly inclined and laminated optical sheet (HILO) microscopy, using a 561nm laser line at 20% laser intensity with an inverted Nikon TiE using a CFI Plan Apo total internal reflection fluorescence 100x 1.49 N.A. objective (Nikon) and ILAS2 targeted laser illumination (Cairn Research). Images were acquired using a Photometrics Evolve Delta EM-CCD camera and Metamorph software (Molecular Devices) at a frame rate of 0.25 seconds with 100ms exposure time for 12.5 mins, or until complete photobleaching occurred. Intensity of each puncta over time (I_{small}) was determined manually within a 6x6 pixel ROI using ImageJ. Background was subtracted by measuring the intensity of a larger a 9x9 pixel ROI (I_{big}) that included the ROI for I_{small}. Background subtracted intensity was calculated by the formula:

$$I_{subtracted} = I_{small} - \left(I_{big} - I_{small}\right) \times \frac{A_{big}}{A_{small} - A_{big}}$$

Where, $I_{subtracted}$ is the background subtracted intensity of the puncta, A_{big} is the area of the larger ROI, and A_{small} is the area of the smaller ROI. Steps were identified using a Matlab-based step-detection algorithm (5).

Expression analyses of control and β-actin MBs

For control and different concentration MB expression analyses, RGC axons were randomly selected in the bright-field channel then imaged using the HILO microscopy set-up described in Materials and Methods, and MB puncta per growth cone counted.

Fluorescence Recovery after Photobleaching (FRAP)

Xenopus laevis eye primordia were electroporated with either 2µg/µl β-actin myr-d2EGFP only, or 2µg/µl β-actin myr-d2EGFP plus 50µM MB1 + MB2. After culturing primary RGC axons, as described above, FRAP experiments were performed on an Olympus IX81 inverted microscope equipped with a PerkinElmer Spinning Disk UltraVIEW VoX, with a 60x (NA, 1.30) Olympus silicone oil immersion objective. Images were captured using Volocity 4.3.2 software (PerkinElmer) with an ORCA-Flash4.0 V2 CMOS camera (Hamamatsu). Axons were photobleached with an UltraVIEW PhotoKinesis device (PerkinElmer) using 90% laser power (488 nm laser line) with 20–30 bleach cycles. Relative fluorescent recovery at each time point was calculated as described previously (6).

LEGENDS FOR SUPPLEMENTAL FIGURES AND MOVIES

Figure S1: Imaging β-actin mRNA with MBs. (A) MBs targeting β-actin mRNA show a concentration-dependent increase in fluorescent intensity, demonstrating the signal is directly dependent of amount of mRNA present. Graphs show the change in fluorescent intensity over time upon addition of 0.125, 0.25, 0.5 and 1 μM *in vitro* transcribed β-actin mRNA for (a) MB1, and (b) MB2. Error bars represent S.E.M, n=3 for each condition. (B) Protocol for MB electroporation into stage 28 *Xenopus* eye primordia and subsequent live imaging of β-actin mRNA in growing retinal ganglion cell axons.

Figure S2: A bright field registration script for estimating colocalisation between puncta in non-simultaneous images: schematic demonstrating workflow applied to estimating colocalisation. (A) Images of MBs labelling β-actin mRNA in axons were taken immediately post-fixation, and compared to images of the same axons after performing smFISH against β-actin mRNA. To enable greater clarity in registering images of axons, the bright-field channels were first contrast-enhanced (N. Desprat , personal communication), and denoised using an implementation of the anisotropic diffusion algorithm (7). Such approaches allow the axons to be more accurately registered to one another, as axon morphology becomes more defined in brightfield. In addition to the exact coordinates of the axon within the frame of imaging being slightly different between the two images, substantial deformation was also observed to take place after performing the smFISH protocol (axons could shrink or be stretched due to the heat and extensive washes involved). To register these bright-field images and estimate colocalisation between MB and smFISH puncta, a combination of two methods were found to work best. Firstly, axons were manually registered based on landmark features in the axon, such as branch points, and the coordinates of the smFISH image transformed according to registration in bright-field Secondly, an automated Iterative Closest

Point (ICP) algorithm (8) was applied to points identified in the fluorescent channel after thresholding. The ICP algorithm uses a nearest-neighbour rule to estimate correspondence between points. A transformation is computed based on these correspondences and the procedure is repeated until the stopping criteria is met. We used an advancement of the ICP algorithm (9), which introduces outlier rejection based on thresholding (code obtained from (10). Fluorescent channels in each image were thresholded for spot detection. In the registered images, the ICP distance between puncta in the first and second image after transformation was calculated. Although some puncta in the first image are not assigned matches to puncta in the second, most puncta are matched between images (often with multiple putative matches). For puncta with multiple matches, we took the smallest ICP distance as the most likely, thus creating a 1:1 ratio of matched puncta between images. In the positive control and smFISH:MB images, the cumulative frequency was weighted towards small ICP distance, with 75% of ICP distances being less than 5.0 and 6.0, respectively, whilst in the negative control, 75% of matched puncta lay within an ICP distance of 450, verifying a lack of matching. In order to provide a quantitative estimate of colocalisation, we set an ICP distance threshold of 1. See main text and figures for results.

(B) Stages in brightfield registration allowing automated colocalisation analysis. (1A) Initial brightfield images, first image after fixation (green) and second after performing smFISH (pink), scale bar 20 μm. (1B) MB puncta (green) and smFISH puncta (pink) before brightfield registration. (2) Puncta and axon outlines after initial brightfield registration, image taken after fixation containing β-actin mRNA labelled by MBs (green) and after performing smFISH against β-actin mRNA (pink). (3) Matched puncta after brightfield ICP registration. Unmatched MBs (green), matched MBs (yellow), β-actin mRNA smFISH puncta (pink circles).

Figure S3: MB hybridization to β-actin mRNA does not significantly affect translation. (A) Representative images showing staining against β-actin protein in WT axons and axons electroporated with MBs targeting β-actin mRNA. (B) Quantification of immunofluorescence shows no significant difference in β-actin protein levels between wild-type axons and MB-expressing axons. Mann-Whitney test, n= 85 and 41 axons, respectively. (C) If MBs were inhibitory to translation one would expect a negative correlation between MB and β-actin protein levels. Instead, comparing intensity of IHC against β-actin protein to MB intensity between individual axons shows a slight, but non-significant positive correlation. Line represents best–fit with 95% confidence limits (Pearson r = 0.227, p =0.057). (D) Performing FRAP with a β-actin-D2EGFP protein synthesis reporter construct reveals comparable levels of translation. Images show representative examples of fluorescence recovery after photobleaching, scale bar 10 μm. (E) Quantification of FRAP recovery using β-actin-D2EGFP with or without MBs showed no significant difference (n=*9* for each condition, two-way ANOVA).

Figure S4: β-actin mRNA stoichiometry and copy number in growing axons. (A) Frequency of raw spot intensities upon performing β-actin mRNA smFISH, RNase-A treated axons was used as a negative control against background. Dotted line is cut-off point representing 98% of the negative background spot population. For clarity, the x-axis only extends to 5000 A.U. as no smFISH spot intensities for RNase-A treatment go beyond this point. (B) Normalised β-actin mRNA smFISH spot intensities after subtracting background population. Arrow shows intensity for one β-actin mRNA molecule. (C) Estimated differences in β-actin mRNA stoichiometry upon mRNA degradation after performing smFISH. Compared to our original smFISH copy number estimation, the distribution of β-actin mRNAs per RNP is shown after binomial fitting to account for a large arbitrary degradation constant of 50%. (D) Examples of the range of β-actin mRNA copy number in axons. Blue arrow shows an

example of a single mRNA, red arrow shows highlights multiplexed RNPs. (E) No significant correlation was observed between the size of the growth cone and number of β-actin mRNA within it (Pearson r = 0.09136, *p*=0.366, *n*=100 axons).

Figure S5: Effect of mRNA half life on growth cone enrichment. Graph showing how, according to our mathematical model, the fold increase in growth cone/axon shaft β-actin mRNA density due anterograde and retrograde transport speeds would vary according to mRNA half-life. Error bars are Gaussian error propagation that incorporates 50% error in half-life values.

Figure S6: Experiments accompanying MB methodology. (A) A predicted off-target for MB2 (Fam83h-like mRNA) was further confirmed not to be expressed in *Xenopus* RGC axons through comparing RTPCR using axon-only RNA and RNA extracted from whole *Xenopus* heads. RTPCR for β-actin mRNA was used as a positive control. mRNAs that are known not to expressed in axons (GluR1 and Map2) were used as negative controls for the purity of axonal RNA. (B) No significant difference in MB expression levels within axons is observed when electroporating 50μM versus 25μM of each MB, suggesting we are electroporating at saturating concentrations with 50μM. (C) An example of MB puncta outside the axon (arrow right panel) that can easily be identified as cell debris in brightfield (left panel).

Movie S1: Dynamic movement of β-actin mRNA in axons labelled by MBs. Movie taken at 5 frames per second showing different compartments of the axon and the different types of mRNA trafficking observed, as seen in fig. 4. Scale bar 10μm.

Movie S2: An example of purely diffusive β-actin mRNA movement. Movie taken at 5 frames per second. Left panel is raw data from particle tracking script, right panel is motion type determined by HMM-Bayes script. D = diffusive state. Scale bar 1μm.

Movie S3: An example of diffusive and directed transport. Movie taken at 5 frames per second. Left panel is raw data from particle tracking script, right panel is motion type determined by HMM-Bayes script. D = diffusive state, DV = directed transport state. Scale bar 1µm.

Movie S4: An example of different directed transport states combined with diffusion. Movie taken at 5 frames per second. Left panel is raw data from particle tracking script, right panel is motion type determined by HMM-Bayes script. D = diffusive state, DV1 = first directed transport state, DV2 = second directed transport state. Scale bar 1µm.

REFERENCES

1. Ströhl F, et al. (2017) Single Molecule Translation Imaging Visualizes the Dynamics of Local β-Actin Synthesis in Retinal Axons. *Sci Rep* 7(1):709.

2. Cagnetta R, Frese CK, Shigeoka T, Krijgsveld J, Holt CE (2018) Rapid Cue-Specific Remodeling of the Nascent Axonal Proteome. *Neuron* 99(1):29–46.e4.

3. Bullock SL, Nicol A, Gross SP, Zicha D (2006) Guidance of bidirectional motor complexes by mRNA cargoes through control of dynein number and activity. *Curr Biol* 16(14):1447–1452.

4. Piper M, et al. (2006) Signaling mechanisms underlying Slit2-induced collapse of Xenopus retinal growth cones. *Neuron* 49(2):215–228.

5. Little MA, et al. (2011) Steps and bumps: precision extraction of discrete states of molecular machines. *Biophys J* 101(2):477–485.

6. Shigeoka T, et al. (2016) Dynamic Axonal Translation in Developing and Mature Visual Circuits. *Cell* 166(1):181–192.

7. Perona, P., and, J. Malik. (1990). Scale-Space and Edge Detection Using Anisotropic Diffusion. *IEEE Transactions on Pattern Analysis and Machine Intelligence,*12, 629–639.

8. Besl, P. and McKay, H. (1992). A method for registration of 3-D shapes. *IEEE Transactions on Pattern Analysis and Machine Intelligence,*14(2): 239-256

9. Feldmar, J. and Ayache, N. (1996). Rigid, affine and locally affine registration of free-form surfaces. *Int J Comput Vision* 18, 99–119.

10. Chui, H. and Rangarajan, A. (2003). A new point matching algorithm for non-rigid registration. *Computer Vision and Image Understanding* 89, 114–141.

FIGURE S1

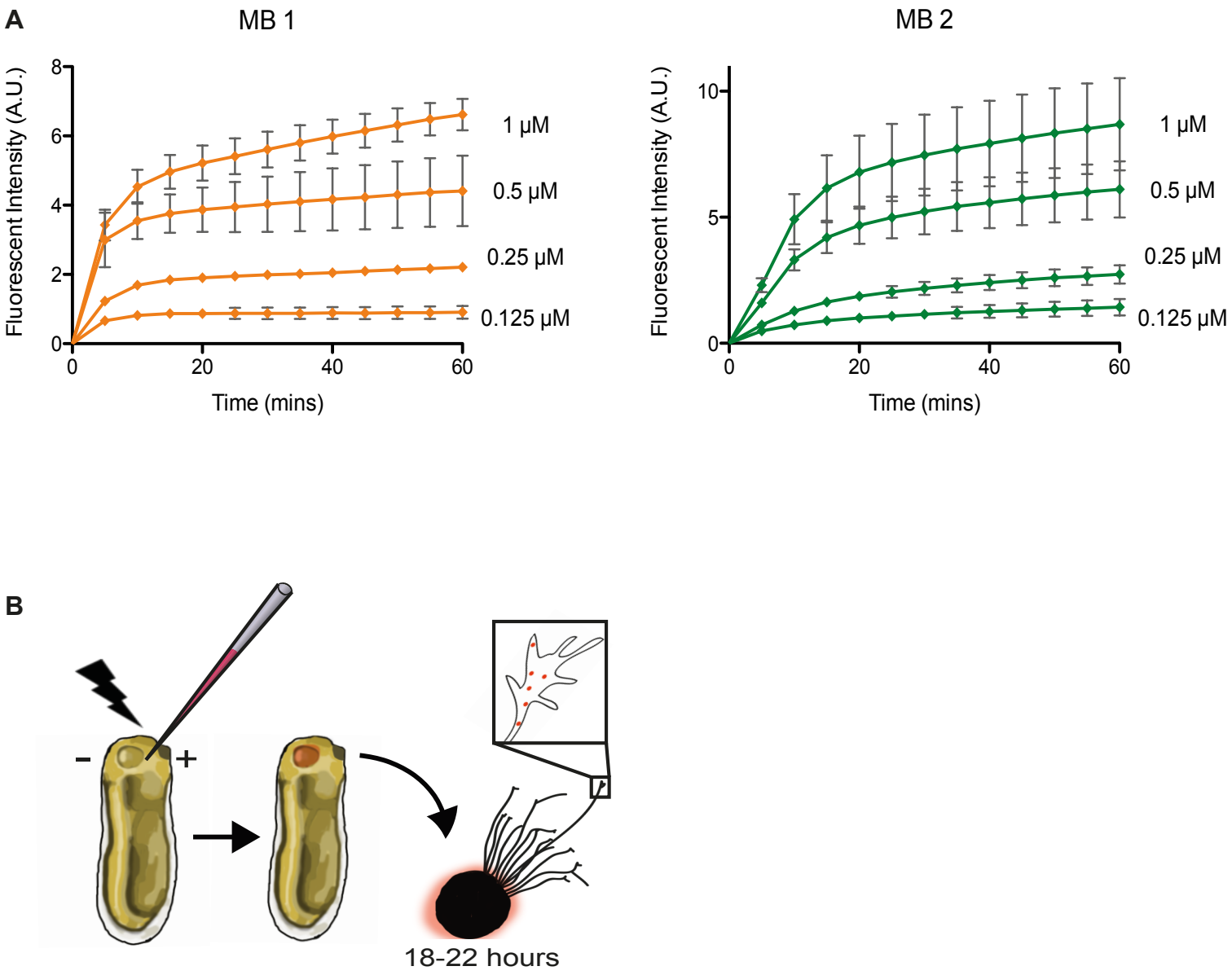
A
MB 1
Fluorescent Intensity (A.U.)
8
6
4
2
0
0
20
40
60
Time (mins)
1 µM
0.5 µM
0.25 µM
0.125 µM
MB 2
Fluorescent Intensity (A.U.)
10
5
0
0
20
40
60
Time (mins)
1 µM
0.5 µM
0.25 µM
0.125 µM
B
–
+
18-22 hours

FIGURE S2

A

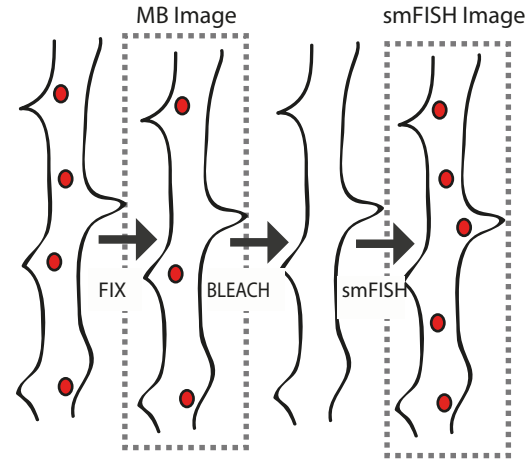

(2) Brightfield Registration

(a) Image Enhancement
-Brightfield contrast enhancement
-Brightfield denoised

(b) 2D spatial transformation (bright field images)
- ROI selection
-Preliminary 2D transformation based on manual point registration

(c) Non-rigid automated point matching (brightfield images)
- Non-rigid point matching of brightfield images based on ICP registration

(d) Transformation of fluorescent images
- smFISH images are transformed according to brightfield transformation from brightfield in the MB image
-Iterated closest point analysis of overlay between MB image and smFISH image

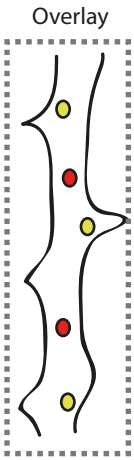

B

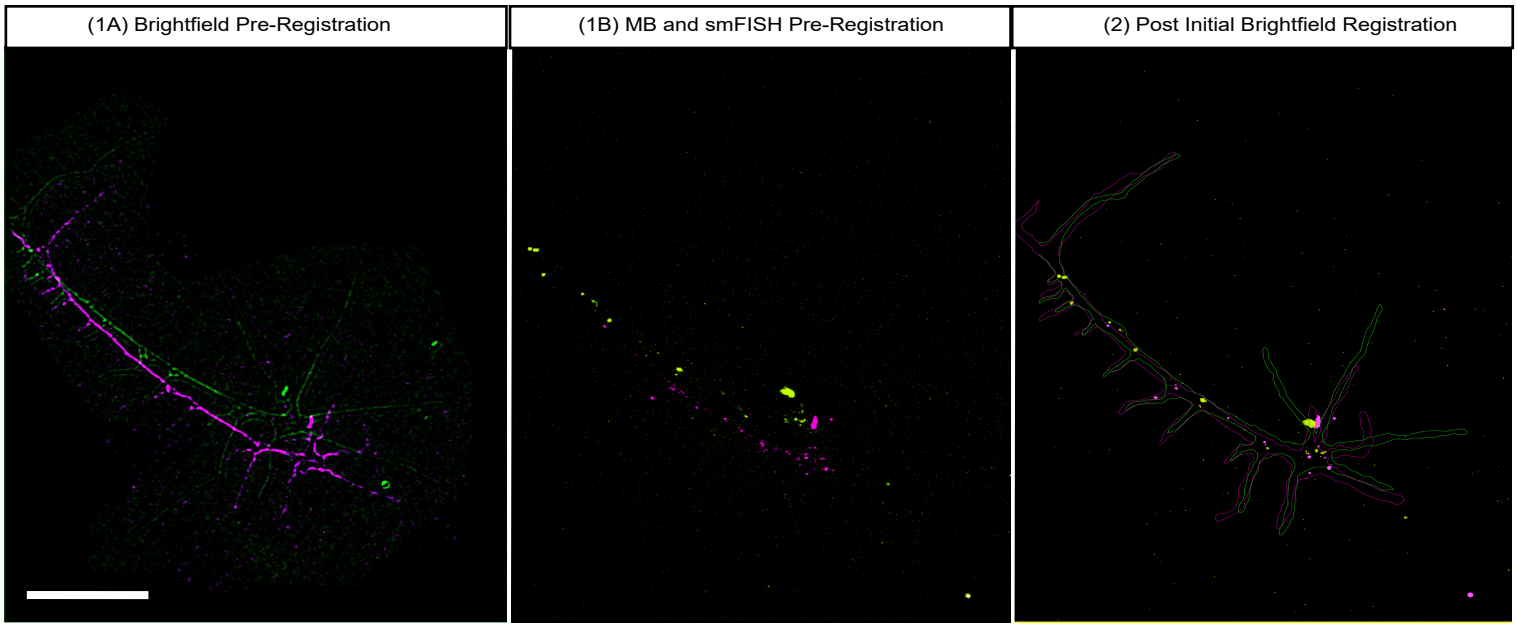

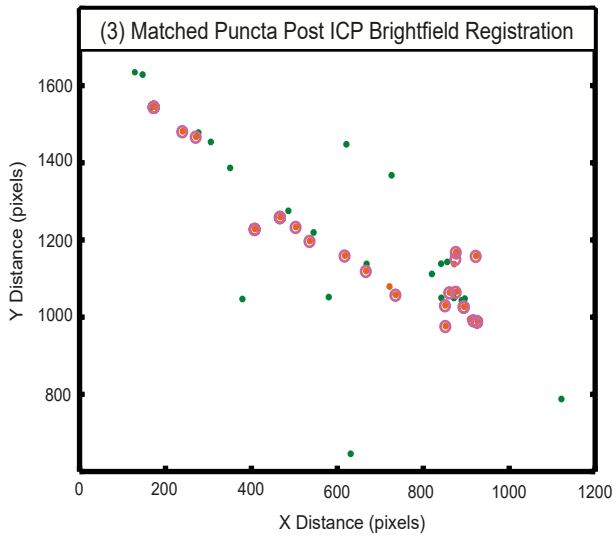

FIGURE S3

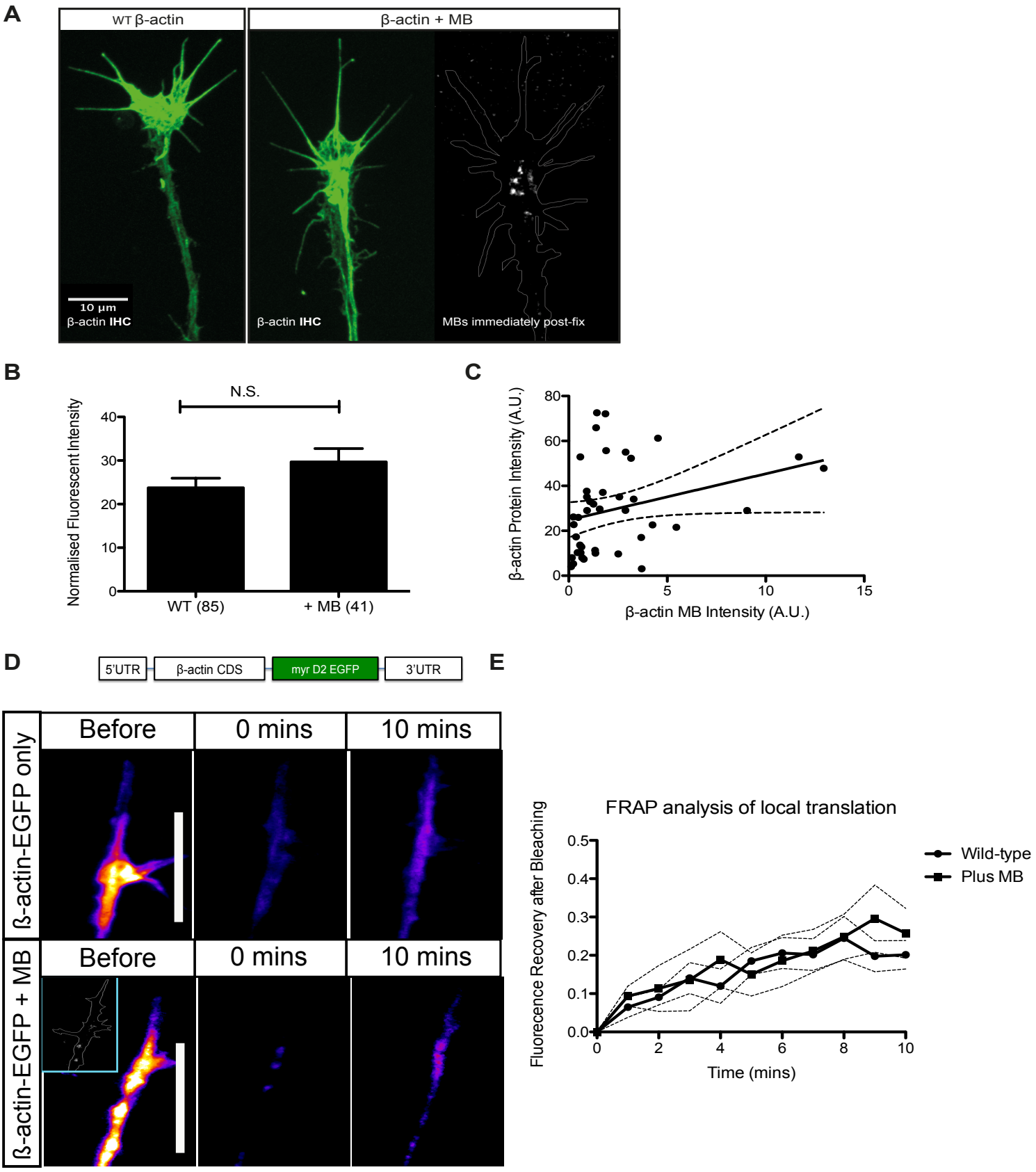
A
WT β-actin
β-actin + MB
10 µm
β-actin IHC
β-actin IHC
MBs immediately post-fix
B
N.S.
Normalised Fluorescent Intensity
40
30
20
10
0
WT (85)
+ MB (41)
C
β-actin Protein Intensity (A.U.)
80
60
40
20
0
0
5
10
15
β-actin MB Intensity (A.U.)
D
5'UTR
β-actin CDS
myr D2 EGFP
3'UTR
E
ß-actin-EGFP only
Before
0 mins
10 mins
ß-actin-EGFP + MB
Before
0 mins
10 mins
FRAP analysis of local translation
Fluorecence Recovery after Bleaching
0.5
0.4
0.3
0.2
0.1
0.0
0
2
4
6
8
10
Time (mins)
Wild-type
Plus MB

FIGURE S4

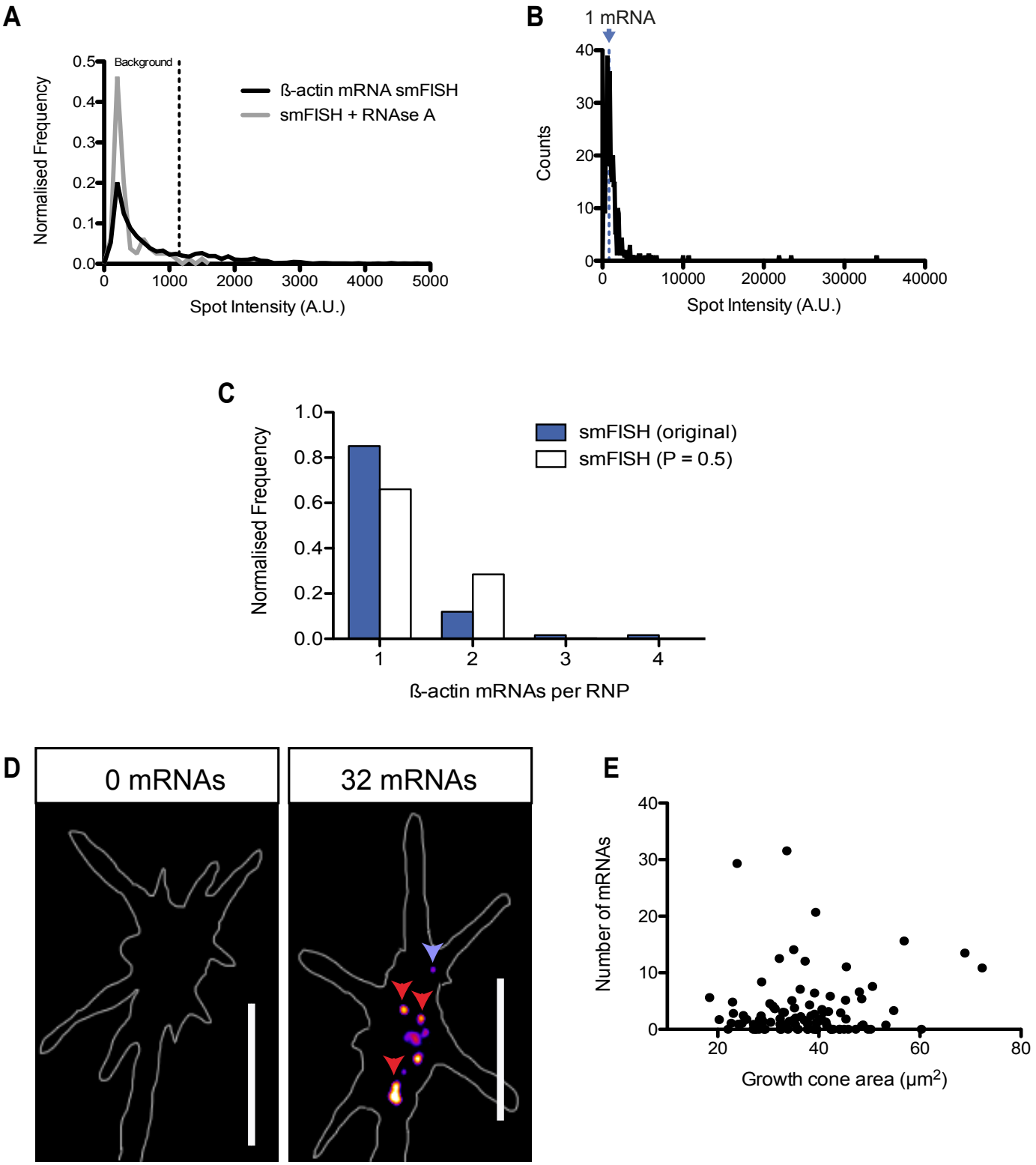
A
Background
ß-actin mRNA smFISH
smFISH + RNAse A
Normalised Frequency
0.5
0.4
0.3
0.2
0.1
0.0
0
1000
2000
3000
4000
5000
Spot Intensity (A.U.)
B
1 mRNA
Counts
40
30
20
10
0
0
10000
20000
30000
40000
Spot Intensity (A.U.)
C
smFISH (original)
smFISH (P = 0.5)
Normalised Frequency
1.0
0.8
0.6
0.4
0.2
0.0
1
2
3
4
ß-actin mRNAs per RNP
D
0 mRNAs
32 mRNAs
E
Number of mRNAs
40
30
20
10
0
20
40
60
80
Growth cone area (µm2)

FIGURE S5

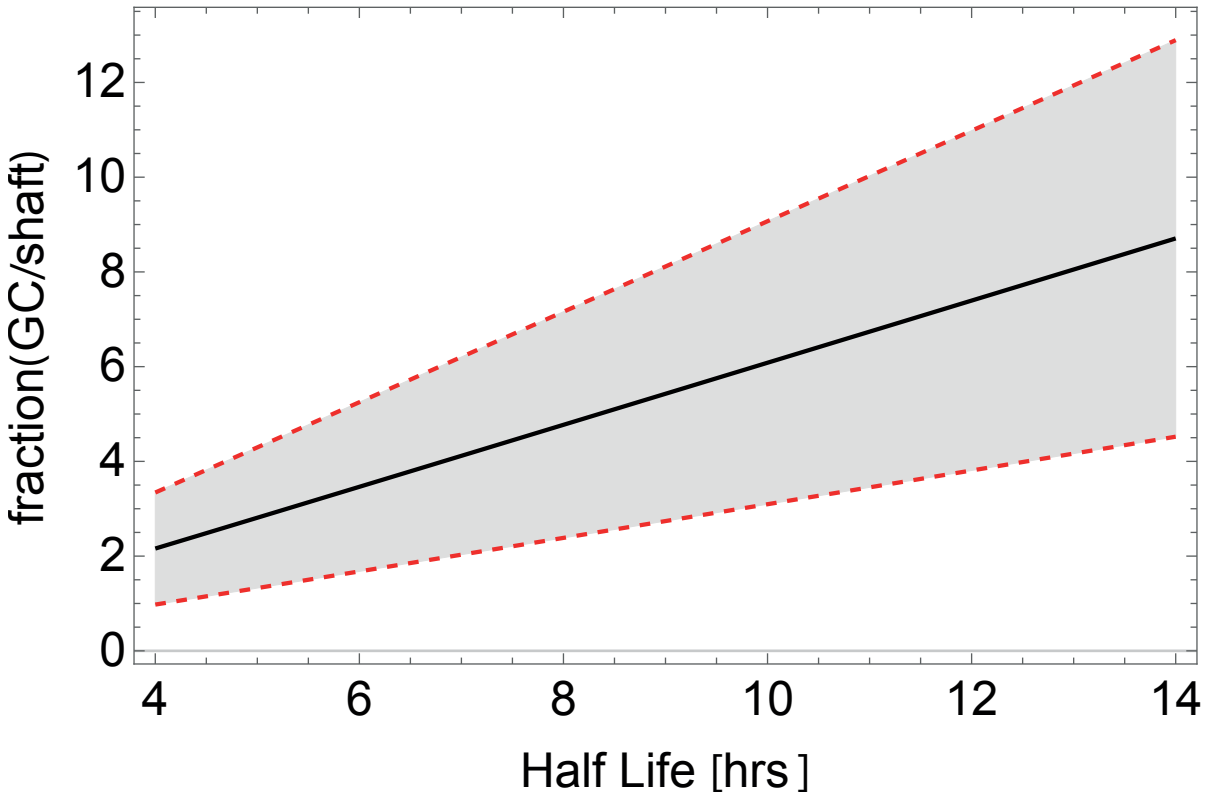

FIGURE S6

A

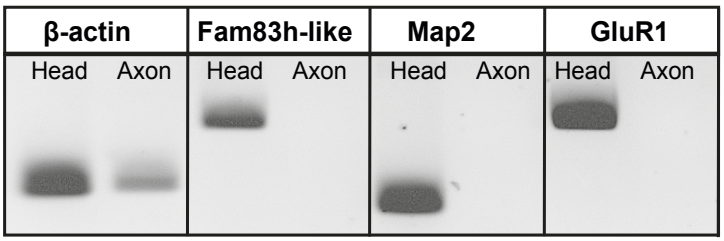

B

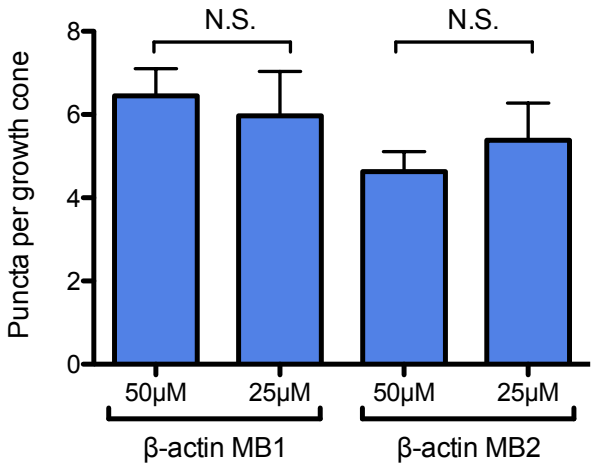

C

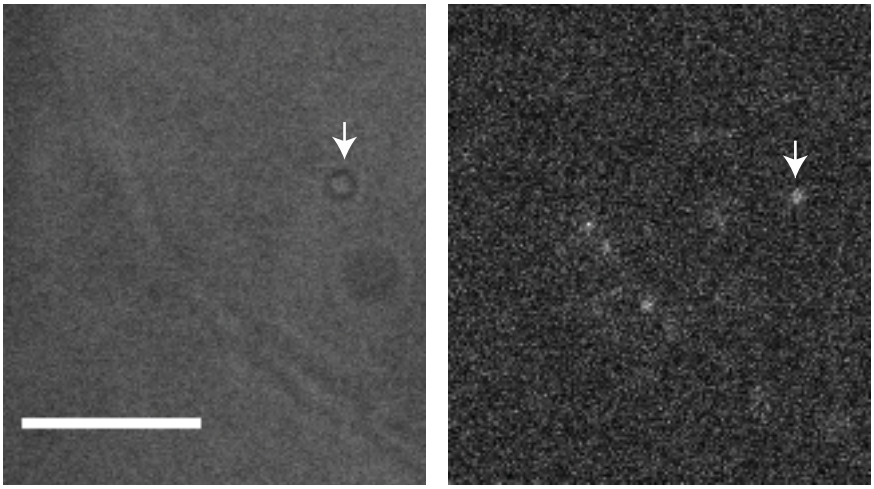

Table S1: smFISH probe sequences used *against X. laevis* β-actin mRNA.

PROBE N^{O}	SEQUENCE 5'-3'	LENGTH
1	AACGACCAGTGCGGCAATAT	20
2	TGCACATACCAGATCCATTA	20
3	AAAACAGCACGGGGAGCATC	20
4	TGGGCGACCCACAATAGATG	20
5	ATCTTTTTGTCCCATTCCAA	20
6	GAGCTTCATCTCCTACATAG	20
7	GTAAGAATACCTCTTTTGCT	20
8	GCCATGTTCAATTGGATATT	20
9	TATCATCCCAGTTGGTGACA	20
10	GTGTGATGCCAGATCTTCTC	20
11	CACTCGCAGTTCATTGTAGA	20
12	CAGCACTGGGTGTTCTTCTG	20
13	GATTCAGGGGTGCTTCTGTG	20
14	ATCTTCTCCCTGTTAGCTTT	20
15	GGTCTCGAACATTATCTGTG	20
16	ACATACATAGCTGGAGTGTT	20
17	GGACAACACAGCTTGGATGG	20
18	TGGTACGACCAGATGCATAC	20
19	CACCTGAGTCCATGACAATA	20
20	ATTGGCACAGTGTGGGTTAC	20
21	TGGTAGAGCATAGCCTTCAT	20
22	CAAGTCCAGACGCAGAATGG	20
23	AGGTAGTCTGTCAGGTCACG	20
24	CCTCTCAGTTAGGATTTTCA	20
25	CTGTGGTGGTGAAGCTGTAC	20
26	TCACGAACGATTTCTCTTTC	20
27	ACATAGCACAATTTCTCCTT	20
28	ATCTCCTGCTCAAAGTCCAG	20
29	TGAAGAAGAGGCAGCTGTGG	20
30	GCTCATAGCTCTTTTCCAAT	20
31	CAATGGTGATGACTTGTCCG	20
32	GGACATCTAAAACGCTCGTT	20
33	AAAGATGGCTGGAAGAGGGC	20
34	AATACCGCAGGATTCCATAC	20
35	TTGAGTTGTAAGTGGTTTCA	20
36	ACGGATATCTACATCACACT	20
37	ACAGTATTGGCATAGAGGTC	20
38	TACATTGTGGTACCACCAGA	20
39	CATTCTATCAGCAATTCCTG	20
40	GCTAGTGCAGTTATTTCTTT	20
41	CTTGATTTTCATGGTGCTGG	20
42	CCAGACAGAGTATTTACGCT	20
43	ACAGGGAAGCCAAGATGGAG	20

44	TGATCCACATCTGCTGGAAG	20
45	CAGACTCATCATACTCCTGC	20
46	TTACGGTGGACAATTGAGGG	20